processes

MDPI

Article

Finite Element Analysis and Improved Evaluation of Mechanical Response in Large Oil Storage Tanks Subjected to Non-Uniform Foundation Settlement

Yuanqi Jiao [1,2], Yanbing Wang [2], Jinzhou Li [2] and Xiaoben Liu [2,*]

[1] National Energy Administration, Beijing 100824, China; jiaoyq2020@163.com
[2] National Engineering Research Center for Pipeline Safety, China University of Petroleum-Beijing, Beijing 102249, China; wangyb4127@163.com (Y.W.); l2326758@126.com (J.L.)
* Correspondence: xiaobenliu@cup.edu.cn

Abstract: This study developed a finite element model to address the issue of non-uniform settlement in large crude oil storage tanks. The model consisted of four key components: the tank foundation, bottom plate, wall plate, and large fillet welds. The Ramberg-Osgood model was used to describe the material's nonlinearity. Key factors such as the radius-to-thickness ratio, height-to-diameter ratio, harmonic number, and amplitude were evaluated for their impact on the radial deformation of the tank's top wall. Two numerical models were developed—one accounting for the coupling effect between the foundation and the tank bottom, and the other without it. The differences in radial deformation between these models were analyzed, revealing that deformation was minimally influenced by the radius-to-thickness ratio, but increased with higher height-to-diameter ratios and harmonic amplitudes. At low liquid levels, radial deformation increased with harmonic number, but at high levels, it decreased once the harmonic number exceeded four due to the decoupling of the tank bottom from the foundation. The model considering foundation coupling exhibited less radial deformation compared to the one neglecting it, particularly as the harmonic number and amplitude increased. An improved evaluation method identified a critical range of harmonic amplitudes for a 100,000 m^3 tank, within which the coupling effect can be reasonably neglected, allowing deformation to be calculated using the simpler model.

Keywords: foundation settlement; storage tank; finite element analysis; harmonic settlement; improved evaluation method

check for updates

Citation: Jiao, Y.; Wang, Y.; Li, J.; Liu, X. Finite Element Analysis and Improved Evaluation of Mechanical Response in Large Oil Storage Tanks Subjected to Non-Uniform Foundation Settlement. *Processes* **2024**, *12*, 2838. https://doi.org/10.3390/pr12122838

Academic Editor: Zheng Sun

Received: 27 October 2024
Revised: 6 December 2024
Accepted: 9 December 2024
Published: 11 December 2024

Copyright: © 2024 by the authors. Licensee MDPI, Basel, Switzerland. This article is an open access article distributed under the terms and conditions of the Creative Commons Attribution (CC BY) license (https://creativecommons.org/licenses/by/4.0/).

1. Introduction

Large oil storage tanks are widely used due to their advantages such as cost-efficiency, reduced land usage, and ease of management, making them important facilities for oil storage and transportation [1–3]. These tanks are generally constructed on homogeneous foundations with sufficient bearing capacity. However, various forms of foundation settlement can occur due to factors such as hydraulic forces, seismic activity, wind loads, and others [4–7]. Additionally, due to the nature of maritime oil trade, many of these tanks are built in coastal areas, which are often characterized by soft soils with high moisture content, significant compressibility, and low bearing capacity, exacerbating foundation settlement issues [8–11]. Numerous studies on incidents involving storage tanks have demonstrated that settlement and instability of oil tanks significantly impact their safe operation [12–18]. To minimize the impact of foundation settlement on the safe operation of storage tanks, further analysis of the deformation behaviour of large storage tanks subjected to non-uniform foundation settlement is necessary.

Scholars have conducted extensive research on the strength analysis of storage tanks subjected to foundation settlement. M. Jonaidi et al. utilized numerical simulation methods to quantitatively study the deformation and stress distribution in large tanks with

varying wall thicknesses under the influence of settlement displacement [19,20]. Sina and Hossein conducted experimental research on localized settlement in tanks with both constant and varying wall thicknesses [21]. Fan et al. analyzed in situ settlement data and developed a settlement prediction model, using finite element methods to quantitatively assess the influence of liquid levels on the buckling strength of storage tanks under settlement displacement [22]. Chen et al. utilized a numerical simulation model to investigate the buckling behaviour of tanks under axial compressive displacement loads, analyzing the variation in critical buckling loads with liquid levels, height-to-diameter ratios, and diameter-to-thickness ratios [23]. Suranga et al. constructed a theoretical analysis model to explore the interaction between soil and the tank base, assuming the soil to be a linearly elastic material. This model quantitatively studied the effects of base width, tank diameter, and the stiffness ratio between the tank base and foundation soil on settlement using finite element methods [24]. In earlier work, M. Jonaidi analyzed the impact of harmonic settlement on tanks with uniform and varying wall thicknesses, revealing that the calculated stress results aligned with experimental data [25]. Several scholars examined the variation in maximum radial deformation of floating roof tank tops and maximum stress on tank bottoms with a harmonic number and geometric parameters of the tank under harmonic settlement through finite element analysis [26–29]. Harsh and Sukru considered the effects of the first five harmonic components to evaluate accumulated damage factors, comparing finite element results with those obtained using methods outlined in API 653. Their study concluded that existing methods may not accurately capture the true deformation of tanks under settlement [30].

Current research on the settlement of large storage tanks mainly focuses on harmonic settlement and non-uniform settlement of tank walls. These studies propose relevant settlement evaluation methods that offer reference value for the development and improvement of related standards. However, it is evident that most existing studies on tank settlement do not account for the interaction between the tank base and foundation. Instead, they generally apply foundation settlement loads directly at the edges of the tank walls, neglecting the coupled effects of soil deformation and the resulting changes in tank stress. In reality, most of the large oil storage tanks are non-anchored, resting freely on reinforced concrete ring beam foundations and relying on friction to maintain stability. Therefore, there is a need for further numerical studies that examine the mechanical response of large oil storage tanks under conditions of a non-uniform foundation settlement.

2. Finite Element Model

2.1. Geometric

Establishing a finite element model using ABAQUS2020. The geometric model of a large crude oil storage tank includes a ring-wall foundation, tank wall, tank floor, and large fillet weld at the joint between the tank wall and the floor. The wall thickness of the storage tank is designed based on the principle of equal strength, with thickness gradually decreasing from the bottom to the top along the height of the tank. For a 100,000 m^3 crude oil storage tank, with a wall height of 21.8 m, variable wall thickness is modelled by setting different shell section thicknesses. The radius of the tank floor is 40 m, and the height and width of the large fillet weld are both set to 13 mm, as referenced in relevant literature. The foundation is modelled using solid elements, with the ring wall of the foundation having a width of 550 mm [31]. The composition and structure of the geometric model for the storage tank and its foundation are shown in Figure 1.

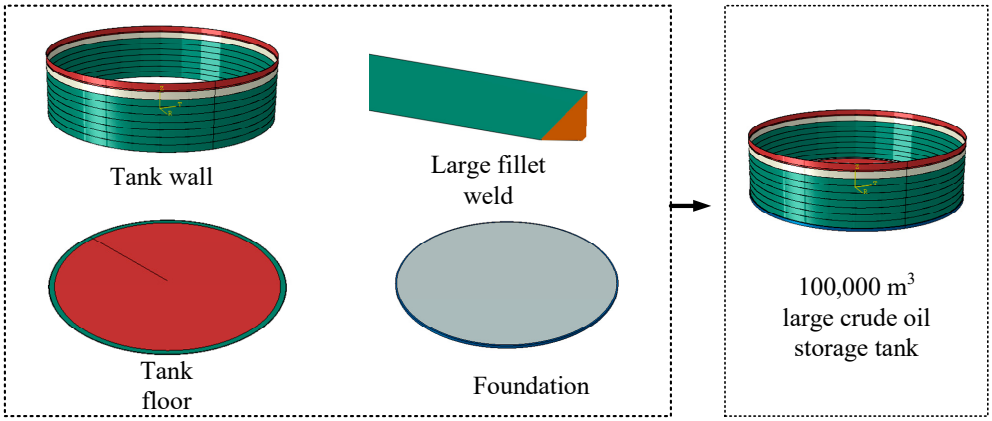


Figure 1. Geometric model of large storage tanks and their components.

2.2. Material

As the tank wall approaches the bottom plate, it bears increasing self-weight and hydrostatic pressure, necessitating higher material strength. To meet these strength requirements, 08MnNiVR steel is used for the bottom edge plate and from the first to the seventh layer of wall plates. The eighth layer of wall plates is made of 16MnR steel, while the ninth layer of wall plates and the middle plates are made of Q235-B steel [32]. The model accounts for material nonlinearity by adopting the Ramberg-Osgood model. The stress–strain relationship curves for these three materials are depicted in Figure 2. The elastic moduli of the reinforced concrete wall and the sandy soil foundation are both set to 2×10^7 Pa.

$$\frac{\varepsilon}{\varepsilon_y} = \frac{\sigma}{\sigma_y} + \alpha\left(\frac{\sigma}{\sigma_y}\right)^m, \tag{1}$$

where ε_y represents the elastic strain at the material's yield point, which is calculated as $\varepsilon_y = \frac{\sigma_y}{E}$; σ_y is the yield stress, MPa; E is the elastic modulus, with E = 206 GPa; α is the hardening coefficient; and m is the power hardening exponent. The material parameters for the storage tank are presented in Table 1.

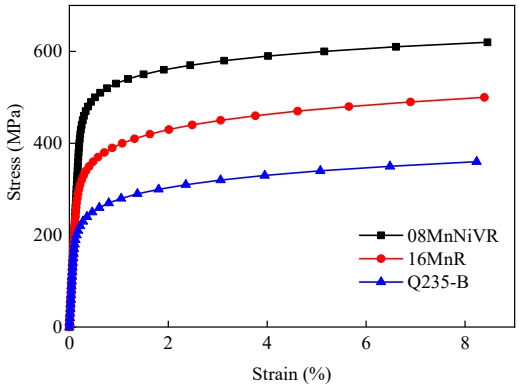


Figure 2. Stress–strain curve of the storage tank material.

Table 1. Material properties of the storage tank components.

Material	Yield Strength/MPa	Hardening Exponent	Power Hardening Exponent
08MnNiVR	490	0.84	15.76
16MnR	345	1.19	10
Q235-B	235	1.75	8.67

2.3. Mesh

The tank wall plates and bottom plates, being typical thin-walled structures, are meshed using 4-node shell elements [33]. The large fillet welds at the joints between the tank wall plates and bottom plate, as well as the ring-wall foundation, are meshed using 8-node solid elements. The meshing result for the 100,000 m^3 large crude oil storage tank is shown in Figure 3. The numerical simulation model consists of 42,780 elements.

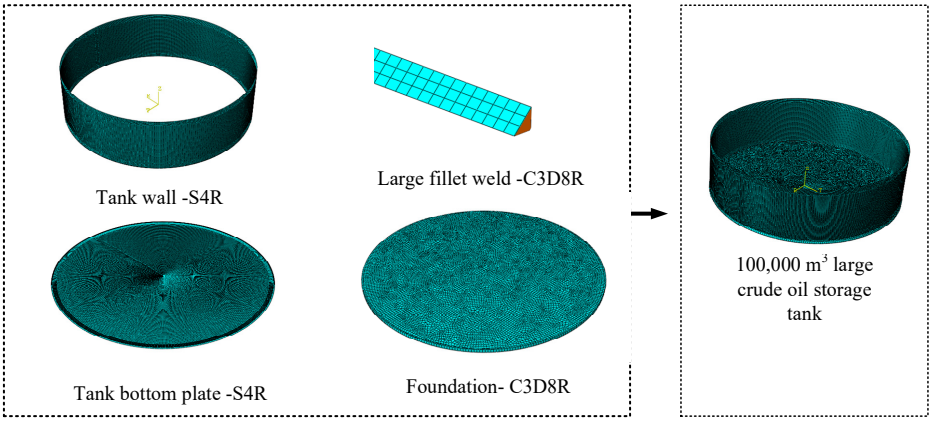


Figure 3. Mesh division of the storage tank and its components.

2.4. Constraint Methods and Boundary Conditions

2.4.1. Model Constraint Methods

The numerical simulation model includes the tank wall plates, bottom plate, foundation, and large fillet weld sections. Tie constraints are established between the contact surfaces of the large fillet weld and the tank wall plates, as well as between the weld and the bottom plate. The tank is a welded structure, tie constraints are applied between the lower surface of the tank wall plates and the upper surface of the bottom plate. The storage tank is usually directly located on the foundation, frictional contact is defined between the lower surface of the tank bottom plate and the upper surface of the foundation, with a friction coefficient of 0.2. A partial view of the tank's large fillet weld structure is shown in Figure 4.

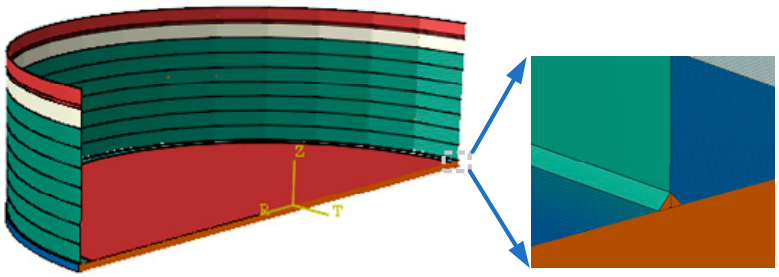


Figure 4. Local structure of the large fillet weld in the storage tank.

2.4.2. Model Boundary Conditions

The initial operational loads on the tank include the self-weight of the tank body and its accessories, as well as the hydrostatic pressure of the stored liquid. Gravitational loads are applied to the entire model. The liquid pressure on the tank wall and bottom plate is calculated using the following formula, gradually decreasing from the tank bottom towards the tank top and forming a triangular distribution. This pressure is applied as uniformly distributed loads to the tank wall and bottom plates. The boundary conditions of the model are shown in Figure 5.

$$p = \rho g(H - h) \quad (2)$$

where p is the hydrostatic pressure, Pa; ρ represents the density of the stored liquid, kg/m^3; g is the gravitational acceleration, N/kg; H is the height of the liquid inside the tank, m; and h is the axial distance from the tank bottom plate, m.

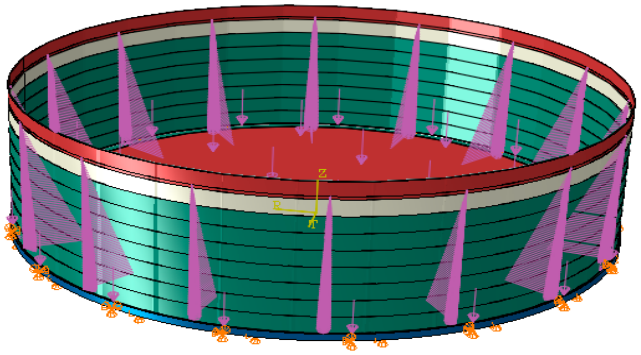


Figure 5. Initial boundary condition setup for the storage tank.

2.5. Verification of the Finite Element Model

The finite element model adopts an implicit solution analysis. A comparative analysis is performed between actual stress test results and the finite element calculation results to verify the accuracy of the finite element model. The relationship between the axial stress on the outer wall of the tank and the tank height, under the combined effects of hydraulic pressure and gravity, is illustrated in Figure 6. The figure shows the measured values of axial and circumferential stresses at a water level of 19.76 m, the finite element calculation results from the literature, and the numerical simulation results from the current model. The variation trends of the curves are generally consistent, and the calculated values for the maximum axial and circumferential stresses are closely aligned. This confirms the accuracy of the finite element model in predicting tank settlement behaviour.

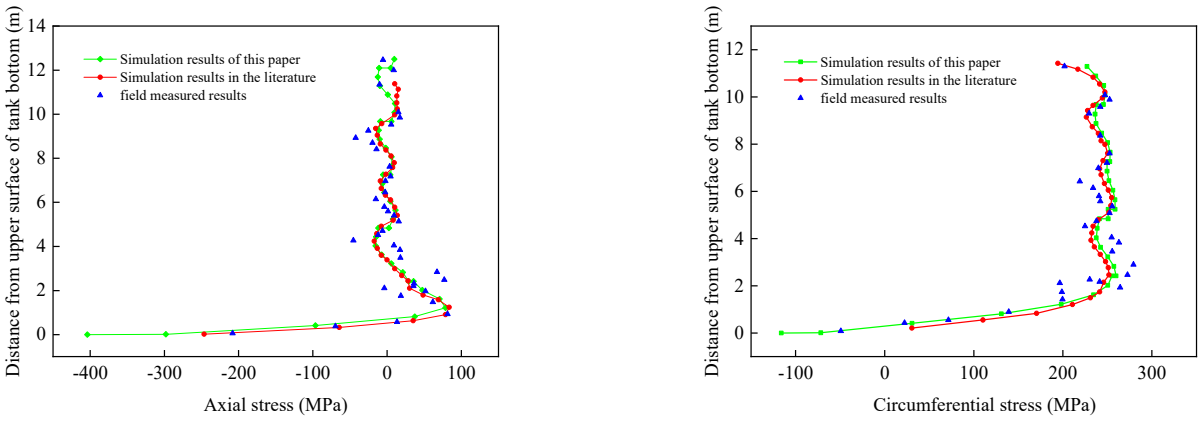


Figure 6. Comparison of calculation results using multiple methods: (**a**) Axial stress; (**b**) Circumferential stress.

3. Numerical Analysis of Large Crude Oil Storage Tanks Under Non-Uniform Ground Loads

3.1. Stress Response Analysis of Storage Tanks on Unsettled Foundations

3.1.1. Stress Response of Tank Wall Panels

Under the initial operational loads of gravity and hydraulic pressure, a large crude oil storage tank undergoes deformations. Using the finite element simulation model of a 100,000 m^3 storage tank, the stress distribution in the tank wall at a liquid level of 19.76 m is calculated and is presented in Figure 7. The computational contour plot shows that axial

stress in the tank wall is primarily concentrated at the junction between the wall and the bottom plate.

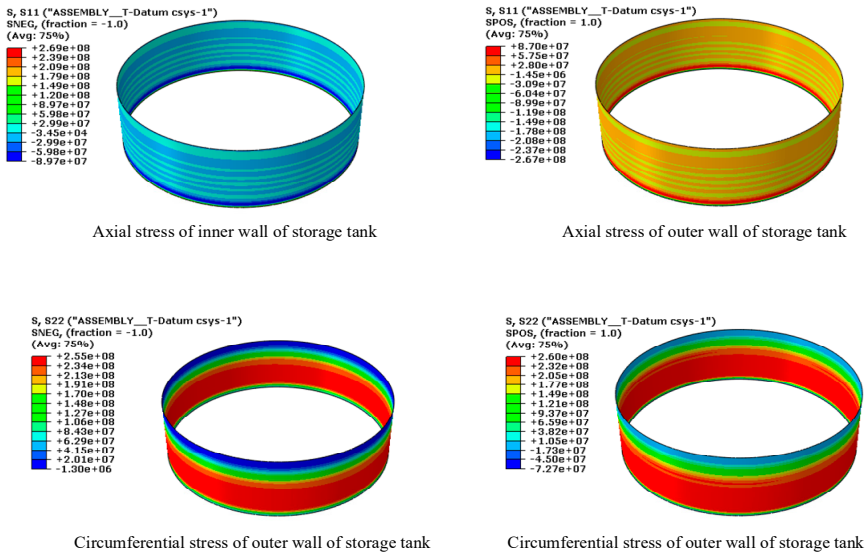


Figure 7. Stress distribution on the tank wall before foundation settlement.

By analyzing the axial and circumferential stresses on both the inner and outer sides of the tank wall at different heights (results shown in Figure 8), it can be observed that the axial stresses on both sides exhibit a symmetrical distribution. Stress concentration occurs at the junction between the tank wall and the bottom plate, which is attributed to variations in wall thickness, leading to fluctuations in axial stress along the height of the tank. Under hydraulic pressure, the circumferential stresses on both sides of the tank wall are relatively similar in magnitude, with the circumferential stress at the large fillet weld being comparatively lower. By calculating the variation in circumferential stress along the tank's height at different liquid levels, as shown in Figure 9, it is evident that the maximum circumferential stress in the tank wall increases continuously as the liquid level rises.

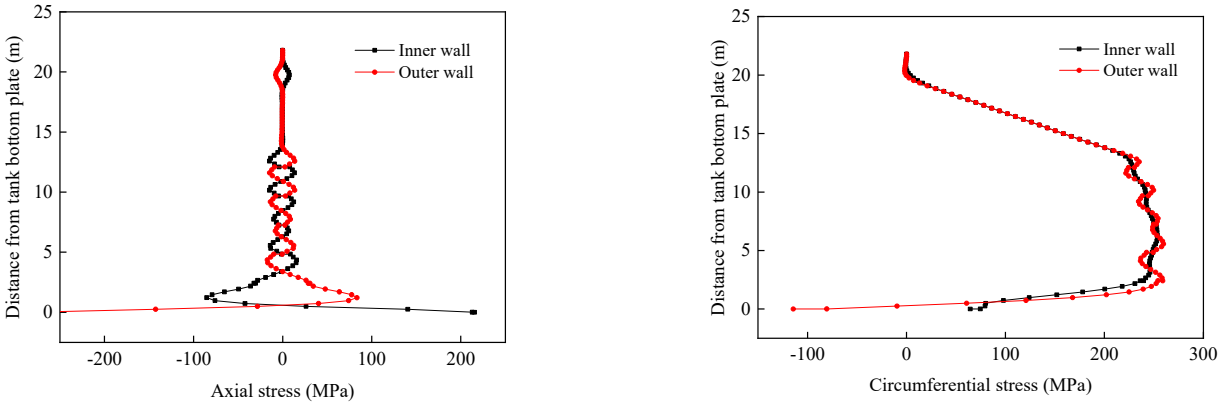


Figure 8. Relationship between wall stress and the height of the storage tank: (**a**) Axial stress; (**b**) Circumferential stress.

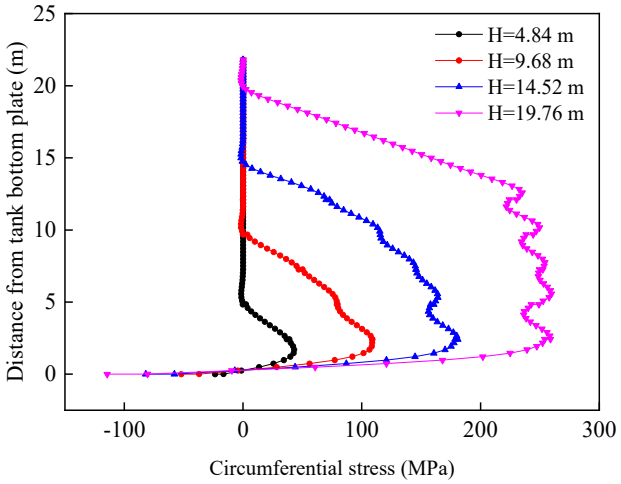


Figure 9. Variation of circumferential stress along the height at different liquid levels.

3.1.2. Stress Response of Tank Bottom Plates

Under the initial operational loads, radial stress dominates on the tank bottom plate, while circumferential stresses remain relatively small. The maximum values of both radial and circumferential stresses are concentrated in the large fillet weld area. The relationship between radial and circumferential stresses on the tank bottom plate, as they vary along the radius of the plate, is illustrated in Figure 10. The black curves represent the results from finite element calculations, while the red curves represent the field-measured values. Both data sets exhibit generally consistent variation trends and similar maximum values, indicating that the use of frictional contact to model the interaction between the tank bottom plate and the foundation is reasonable. This further validates the accuracy of the numerical simulation model.

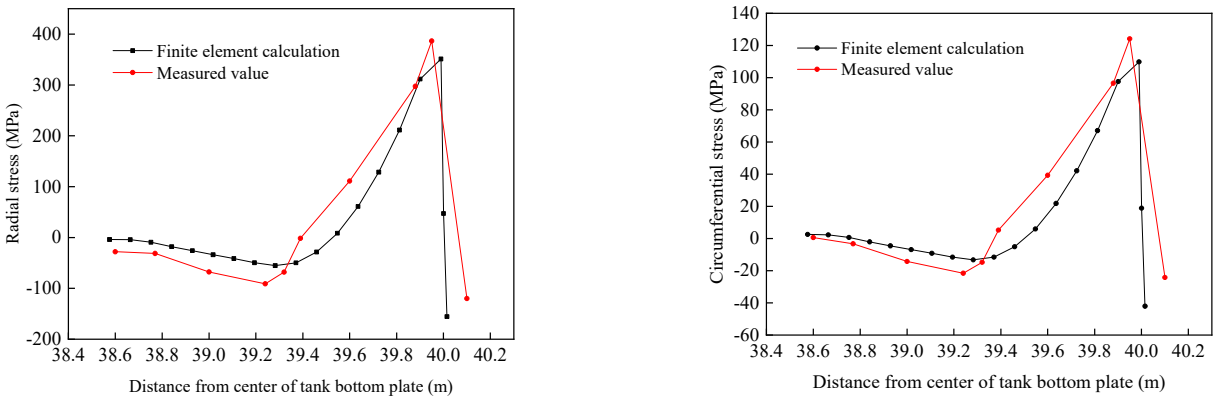


Figure 10. Stress variation curve in a storage tank bottom plate: (**a**) Radial stress of outer wall; (**b**) Circumferential stress of outer wall.

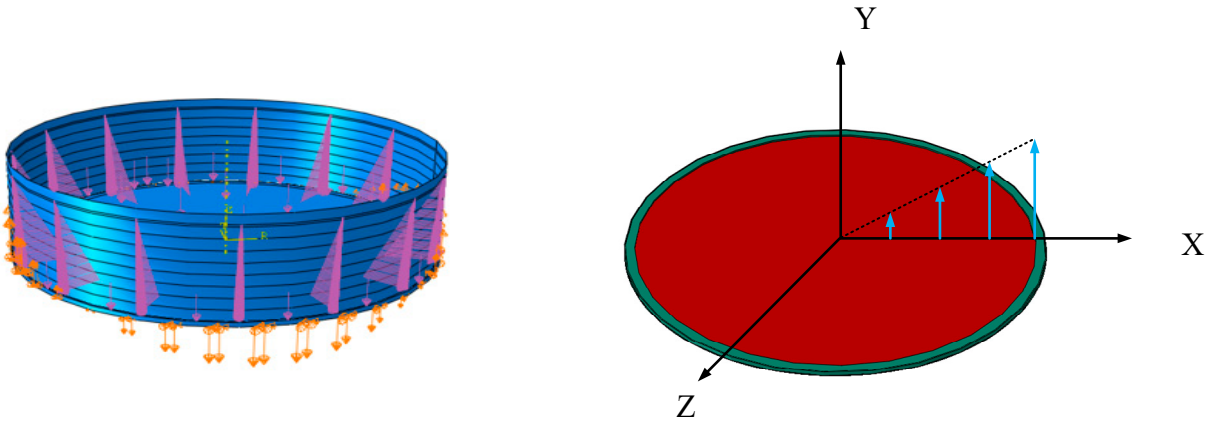
3.2. Load Setting for the Tank Foundation Settlement

Based on the field settlement inspection and monitoring data, a Fourier series is used to fit the measured discrete data of the tank foundation settlement into a form composed of several harmonic components of different orders.

$$\begin{cases} u(\theta) = u_0 + \sum_{n=1}^{k} (u_{c,n}\cos(n\theta) + u_{s,n}\sin(n\theta)) \\ u_0 = \frac{1}{N}\sum_{i=0}^{N-1} u(\frac{2\pi}{N}\cdot t) \\ u_{c,n} = \frac{2}{N}\sum_{i=0}^{N-1} u(\frac{2\pi}{N}\cdot t)\cdot\cos(n\cdot\frac{2\pi}{N}\cdot t) \\ u_{s,n} = \frac{2}{N}\sum_{i=0}^{N-1} u(\frac{2\pi}{N}\cdot t)\cdot\sin(n\cdot\frac{2\pi}{N}\cdot t) \end{cases} \quad (3)$$

where i represents the number of measurement points; N is the total number of measurement points; n denotes the number of harmonics; θ is the circumferential angle of the tank bottom when unfolded; and u_0 is the uniform settlement amount.

The tank settlement load is divided into a single harmonic settlement and an uneven foundation settlement. The axial displacement of the outer edge nodes of the foundation is calculated using the Fourier series expression. The boundary conditions for the tank under a single harmonic settlement are depicted in Figure 11. The circumferential and radial deformations of the nodes on the lower surface of the tank foundation are set to zero. The axial displacement of the outer edge nodes is set according to the settlement amount, represented by a combination of harmonics or a single harmonic using the Fourier series. The axial displacement of the central node is defined as the average of the axial displacements of the outer edge nodes, while the axial displacement of the remaining nodes varies linearly along the radial direction.



(**a**) (**b**)

Figure 11. Boundary conditions setup for the storage tank under the single harmonic settlement: (**a**) The entire model load condition; (**b**) distribution of settlement load on a tank floor.

3.3. Analysis of Factors Influencing the Mechanical Response of a Storage Tank

3.3.1. Diameter-to-Thickness Ratio

Under the same foundation settlement, changes in the geometric dimensions of the tank body significantly affect its deformation response. Keeping the outer diameter of the tank wall constant, the diameter-to-thickness ratio (D/T) is varied by adjusting the thickness of the tank wall plates, while maintaining the same ratio between the thicknesses of the various wall layers. This approach references the range of D/T values found in relevant literature [34]. The specific calculation conditions and parameters are shown in Table 2. Additionally, the influence of the liquid level on the deformation of the tank body is analyzed.

Table 2. Calculation conditions for different diameter-to-thickness ratios.

Operating Parameters	Harmonic Amplitude/mm	Harmonic Number	Height-to-Diameter Ratio	Diameter-to-Thickness Ratio	Liquid Level/m
Value	40	3	0.5	500, 800, 1200, 1500, 1700, 2000	0, 9.68, 19.76

As shown in Figure 12, when the tank liquid level is 19.76 m, the radial deformation at the top of the tank wall increases as the D/T increases. At different liquid levels, the radial deformation at the trough position of the top of the tank wall remains almost unchanged with increasing D/T, showing only millimetre-scale variations. Figure 13 indicates that the liquid level has a relatively small impact on the radial deformation of the tank wall. This suggests that for large tanks in normal service, changes in wall thickness have a minor influence on the radial deformation of the tank under harmonic settlement.

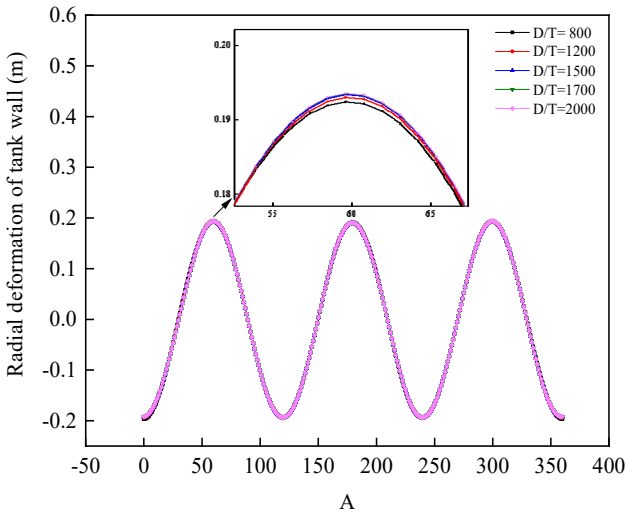


Figure 12. Relationship between radial deformation of the tank wall and circumferential unfolding angle under different diameter-to-thickness ratios.

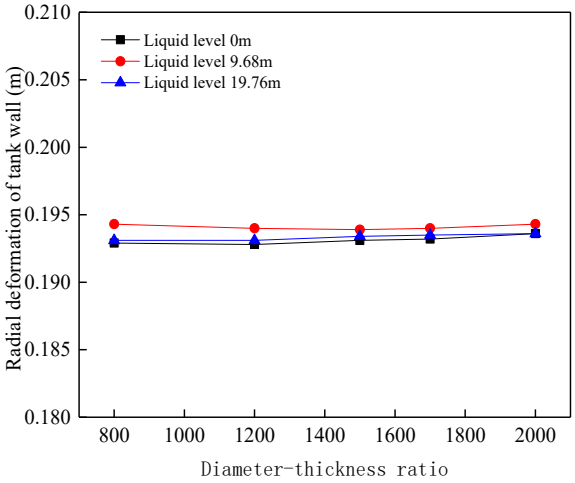


Figure 13. Relationship between radial deformation of the tank wall and the diameter-to-thickness ratio at different liquid levels.

3.3.2. Height-to-Diameter Ratio

The height-to-diameter ratio (H/D) of a tank is defined as the ratio of the tank's height to its outer diameter. As the tank's height increases, the stiffness and stability of the tank

under foundation settlement undergo significant changes. To investigate the deformation response of tanks with different aspect ratios under a specific single harmonic settlement, the outer diameter is fixed at 80 m. By adjusting the tank's height and referencing the range of aspect ratios found in the relevant literature [30], the deformation response of the tank under different aspect ratios is calculated. The specific calculation conditions and parameters are shown in Table 3.

Table 3. Calculation conditions for different height-to-diameter ratios.

Operating Parameters	Harmonic Amplitude/mm	Harmonic Number	Height-to-Diameter Ratio	Diameter-to-Thickness Ratio	Liquid Level/m
Value	40	3	0.5, 0.8, 1.0, 1.5	2200	0, 9.68, 19.76

As shown in Figures 14 and 15, the radial deformation at the top of the tank wall increases as the H/D increases. At different liquid levels, the radial deformation at the top of the tank wall increases approximately linearly with the aspect ratio. This occurs because, with a fixed tank diameter, as the tank height increases, stability decreases, making the top of the tank wall more susceptible to deformation. The influence of the liquid level on radial deformation at the top of the tank wall is relatively small, and from an engineering perspective, it can be considered negligible. Under the same foundation settlement, reducing the H/D appropriately can help decrease the deformation at the top of the tank wall.

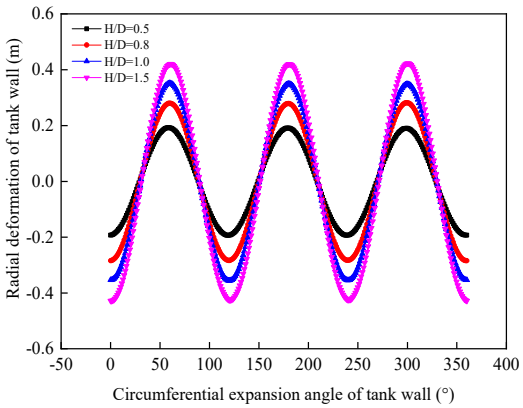


Figure 14. Relationship between radial deformation of the tank wall and circumferential unfolding angle under different height-to-diameter ratios.

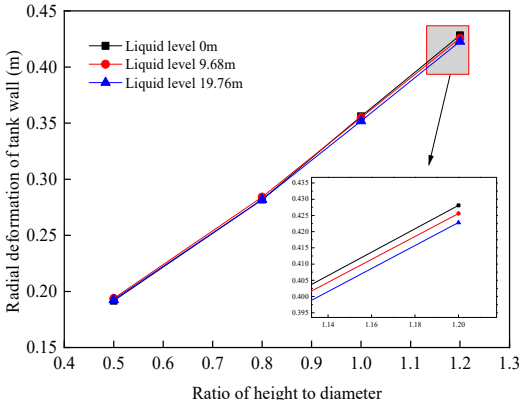


Figure 15. Relationship between radial deformation of the tank wall and the height-to-diameter ratio at different liquid levels.

3.3.3. Harmonic Number

The uneven settlement curve of the foundation can be decomposed into several single harmonic settlements using the Fourier series. Harmonic settlements up to the sixth harmonic, accurately reflect the true state of uneven foundation settlement. Specifically, harmonic settlements with $N = 0$ and $N = 1$ represent overall uniform settlement and planar tilt settlement of the tank, respectively. With the harmonic amplitude set at 40 mm, the deformation response of the tank under different harmonic numbers and liquid levels is calculated. The specific calculation conditions and parameters are shown in Table 4.

Table 4. Calculation conditions for different harmonic numbers.

Operating Parameters	Harmonic Amplitude/mm	Harmonic Number	Height-to-Diameter Ratio	Diameter-to-Thickness Ratio	Liquid Level/m
Value	40	2, 3, 4, 5, 6	0.5	2200	0, 9.68, 19.76

As illustrated in Figure 16, for different harmonic numbers, the radial deformation of the tank wall exhibits a periodic symmetrical distribution around the circumference of the tank, with the number of periods matching the harmonic number. Figure 17 demonstrates that at low liquid levels, the maximum radial deformation of the tank wall increases as the harmonic number increases. At this stage, the tank bottom plate remains fully in contact with the foundation. As the harmonic number increases, the same vertical displacement must occur over a smaller circumferential width, leading to progressively greater deformation of the tank. However, when the tank is full, the deformation of the tank body first increases and then decreases. This is because the liquid inside the tank generates significant circumferential stress on the tank wall, which enhances the overall stiffness of the tank, as illustrated by the contour plot in Figure 18. Consequently, when the harmonic number exceeds four, the tank bottom plate separates from the foundation. After this separation, an increase in the harmonic number results in more circumferential support points for the tank, leading to a reduction in deformation.

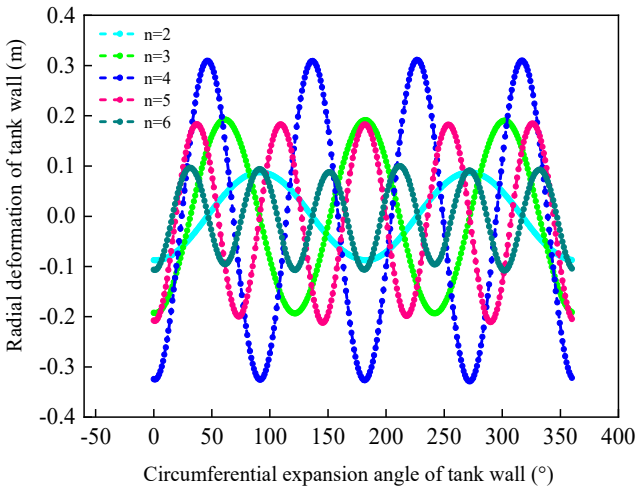


Figure 16. Relationship between radial deformation of the tank wall and circumferential unfolding angle under different harmonic numbers.

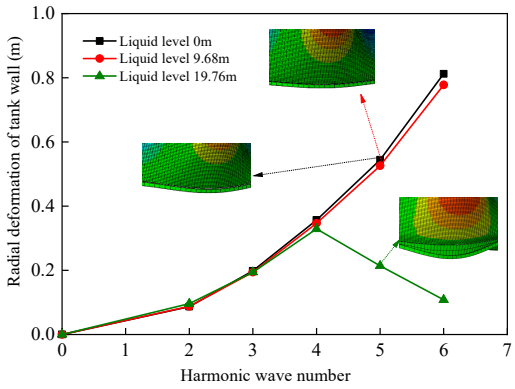


Figure 17. Relationship between radial deformation of the tank roof and harmonic numbers at different liquid levels.

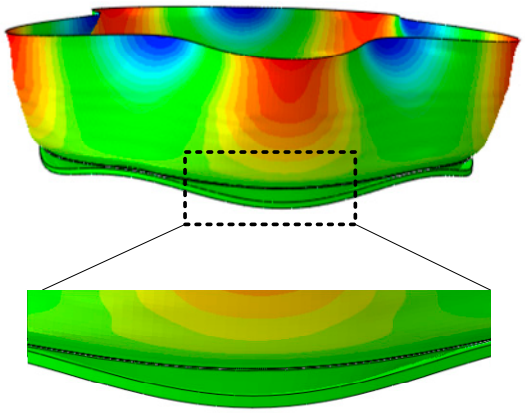


Figure 18. Schematic diagram of local separation between the tank bottom and foundation.

3.3.4. Harmonic Amplitude

Based on field test data of uneven tank foundation settlement, it is observed that low-order harmonic components tend to have relatively large amplitudes, and the amplitudes of individual harmonic settlements at various orders reflect the actual settlement pattern of the tank to some extent. Harmonic amplitude has a significant impact on the deformation response of the tank under a single harmonic settlement. With the harmonic number set to three, the deformation response of the tank under different harmonic amplitudes and liquid levels is calculated. The specific calculation conditions and parameters are shown in Table 5.

Table 5. Calculation conditions for different harmonic amplitudes.

Operating Parameters	Harmonic Amplitude/mm	Harmonic Number	Height-to-Diameter Ratio	Diameter-to-Thickness Ratio	Liquid Level/m
Value	20, 40, 60, 80, 100	3	0.5	2200	0, 9.68, 19.76

As shown in Figure 19, the radial deformation at the top of the tank wall increases as the harmonic amplitude increases. The radial deformation of the tank wall exhibits a periodic symmetric distribution along the circumference of the tank. Figure 20 illustrates that, with a harmonic number of three, the radial deformation of the tank wall at the trough position increases linearly with the rise in harmonic amplitude. This is because, when the harmonic number is three, there is no separation between the tank bottom plate and the foundation, causing the tank wall to be more significantly affected by foundation settlement as the harmonic amplitude increases. Regardless of the harmonic amplitude, the influence of the liquid level on the radial deformation of the tank wall remains negligible.

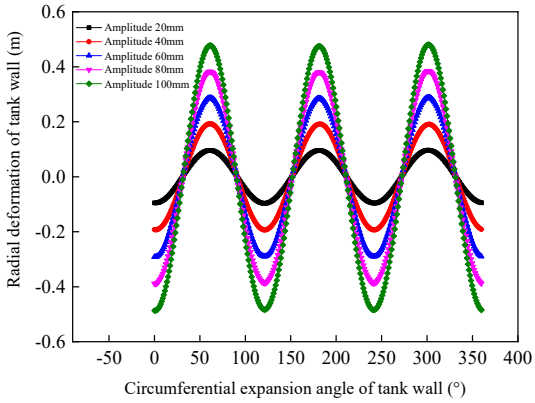


Figure 19. Relationship between radial deformation of the tank wall and its circumferential unfolding angle under different harmonic amplitudes.

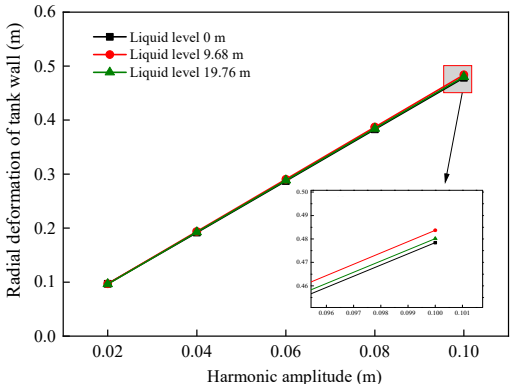


Figure 20. Relationship between radial deformation of the tank wall and harmonic amplitude at different liquid levels.

4. Improved Evaluation Method for Storage Tanks Subject to Uneven Foundation Settlement

4.1. Influence of Foundation on the Nonlinear Response of Storage Tank Structures

As shown in Figure 21, the variation in uneven settlement around the tank perimeter foundation is obtained from field test data. The radial deformation of the tank wall is calculated for two numerical simulation models: one considering foundation–tank interaction and the other neglecting it. As illustrated in Figure 22, the radial deformation of the tank wall is smaller in the model considering foundation–tank interaction, due to the separation between the foundation and the bottom plate, compared to the symmetrical model that does not consider the foundation.

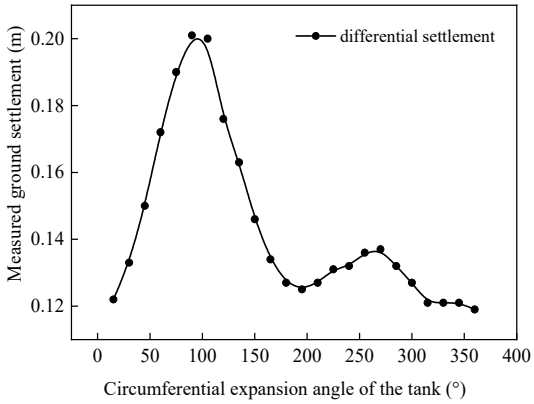


Figure 21. Measured uneven settlement values of tank foundation.

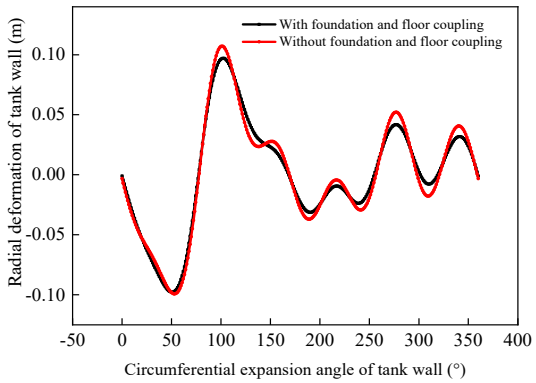


Figure 22. Variability in model results.

The numerical simulation model for large crude oil storage tanks that considers foundation–tank interaction exhibits multiple nonlinearities, making it inconsistent with the principle of superposition. Consequently, the calculation results for single harmonic settlement cannot be fully applied to the analysis of uneven foundation settlement. To evaluate the influence of foundation–tank bottom plate interaction on single harmonic settlement, the difference in radial deformation of the tank wall is analyzed between the two numerical simulation models—one considering foundation–tank interaction and the other not—across different harmonic numbers and amplitudes.

4.1.1. Influence of Harmonic Number on the Variability of Mechanical Response Results

With the harmonic amplitude set to 40 mm and the tank liquid level at 19.76 m, the radial deformation of the tank wall is calculated for two numerical simulation models: one considering the foundation–tank interaction and the other excluding it, across various harmonic numbers. Relationship curves showing the differences in the calculation results between the two models as a function of the circumferential angle along the tank wall are plotted for different harmonic numbers. As shown in Figure 23, the difference in radial deformation between the two models increases with the rise in harmonic numbers.

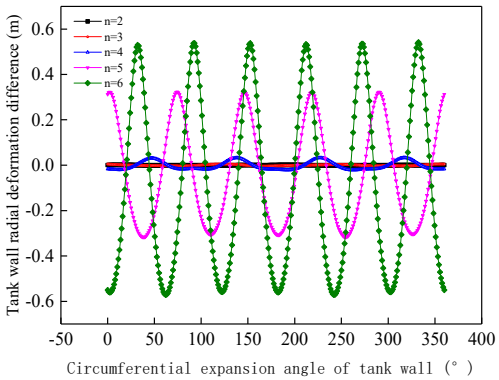


Figure 23. Relationship between result differences and circumferential unfolding angle of the tank wall under different harmonic numbers.

4.1.2. Influence of Harmonic Amplitude on the Variability of Mechanical Response Results

With the harmonic number set to three and the tank liquid level at 19.76 m, the radial deformation of the tank wall is calculated for two numerical simulation models: one considering the foundation–tank interaction and the other not considering it, across different harmonic amplitudes. Relationship curves, showing the differences in calculation results between the two models as a function of the circumferential angle along the tank wall, are plotted for various harmonic amplitudes. As shown in Figure 24, the discrepancy in radial deformation between the models increases as the harmonic amplitude rises.

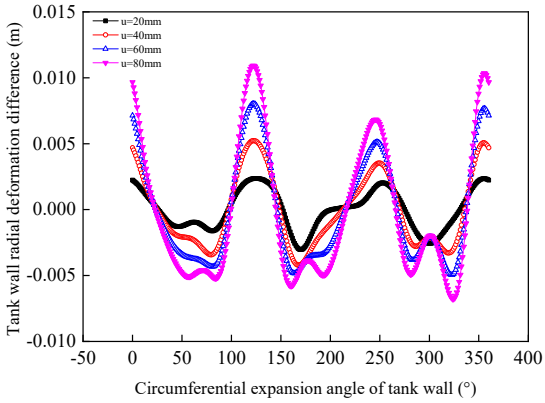


Figure 24. Relationship between differences in two numerical simulation results and circumferential unfolding angle of the tank wall.

4.2. Research on Improvement Evaluation Method for Tank Deformation

To determine the error range within which the influence of the foundation on tank wall deformation can be considered negligible under specific conditions of uneven ground settlement, a critical harmonic amplitude is proposed for single-harmonic settlement. When the harmonic settlement amplitude is less than this critical value, the error in tank wall deformation caused by foundation influence is considered insignificant. Based on the principle of superposition of tank deformation, the deformation response of tank walls under uneven settlement loads from the foundation is analyzed using the computational results of a single-harmonic settlement. This approach simplifies the process of analyzing tank deformation responses under settlement loads, reducing computational complexity.

To calculate the Root Mean Square Error (RMSE) between the estimated and true values of tank wall deformation under settlement from each harmonic component (N = 2 to 6), and to identify the critical harmonic amplitude for the single-harmonic settlement, the following specific calculation formulas are applied. The estimated value refers to the tank wall deformation without considering the foundation influence for a given harmonic settlement, while the true value represents the tank wall deformation when foundation coupling is included under the same harmonic settlement. The detailed calculation formulas are as follows:

$$RMSE = \sqrt{\frac{1}{N}\sum_{i=1}^{N}(u_{i,true} - u_{i,estimate})^2}, \tag{4}$$

where N represents the number of test points; $u_{i,true}$ denotes the true value of the tank deformation at the i-th test location; and $u_{i,estimate}$ denotes the estimated value of the tank deformation at the i-th test location.

As shown in Figure 25, based on the numerical simulation model for the deformation response of storage tanks under uneven settlement, relationship curves are plotted to illustrate how the error values between the approximately estimated radial and circumferential deformations of the tank and the true deformation values vary with harmonic amplitudes.

The critical harmonic amplitude that satisfies the error requirements for the deformation of a storage tank wall under a single harmonic settlement is denoted as $U_{critical}$. When each harmonic settlement amplitude from the uneven foundation settlement displacement curve, derived through Fourier series expansion, is less than its corresponding critical harmonic amplitude $U_{i,critical}$, the deformation of the storage tank wall can be approximately estimated using the results from a model that excludes foundation effects. The specific criterion is given by the following formula:

$$U_i \leq U_{i,critical} \quad 1 \leq i \leq n, \tag{5}$$

where n represents the harmonic number; U_i denotes the amplitude of the i-th harmonic; and $U_{i,critical}$ represents the critical harmonic amplitude for the i-th harmonic.

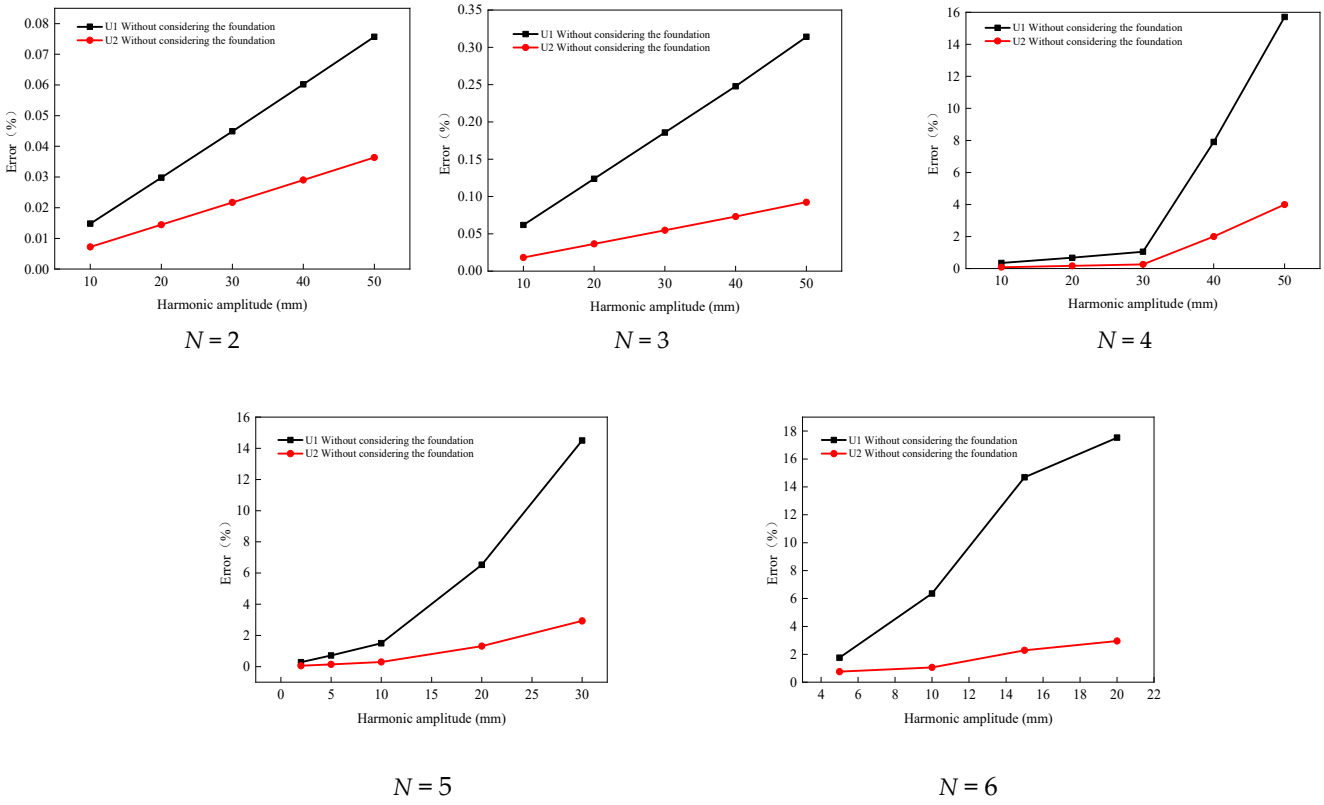


Figure 25. Relationship between deformation error of the tank wall and harmonic amplitude under different harmonic numbers.

When setting the maximum error for the radial deformation U_1 of the storage tank wall due to neglecting foundation effects to 10%, and the maximum error for the circumferential deformation U_2 to 1%, the critical harmonic amplitudes that meet these error requirements for different harmonic numbers are shown in Figure 26.

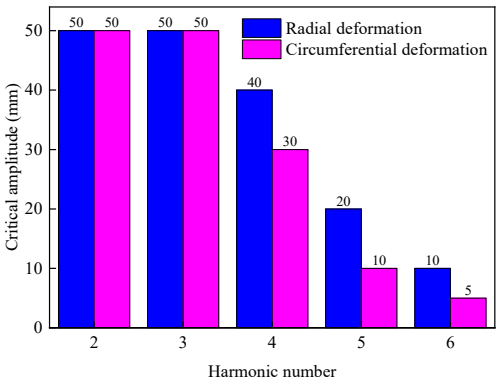


Figure 26. Distribution of critical harmonic amplitudes for tank wall deformation within error limits.

5. Conclusions

Based on the numerical simulation model of large crude oil storage tanks, this study quantitatively analyzes the influence of the tank wall's D/T, H/D, harmonic number, and harmonic amplitude on the radial deformation and axial stress of the tank wall. The following conclusions are drawn:

(1) By considering the coupling between foundation settlement and tank stress response under real service conditions, a mechanical simulation model for deformation analysis of large storage tanks subjected to uneven foundation settlement is established. The axial stress distribution in the tank wall, induced by hydraulic pressure and gravity, is calculated. The accuracy of the numerical simulation model is verified through a comparative analysis with field test data.

(2) The radial deformation at the top of the tank wall is relatively less affected by the D/T and liquid level. It increases approximately linearly with the H/D and harmonic amplitude. Under low liquid level conditions, the radial deformation at the top of the tank wall increases with the harmonic number. Under high liquid level conditions, the radial deformation initially increases with harmonic number, but once the harmonic number reaches a point where the bottom plate separates from the foundation, the radial deformation decreases with further increases in harmonic number.

(3) The differences in the calculation results between tank numerical models that include or exclude foundation effects are analyzed, leading to an improved method for evaluating tank deformation. By quantitatively analyzing the influence of the harmonic number and amplitude on the mechanical response differences in the tank wall, this study provides estimates of the deformation errors resulting from neglecting foundation effects for harmonic numbers ranging from two to six and varying harmonic amplitudes for 100,000 m^3 large storage tanks. Additionally, the critical range of harmonic amplitudes that meet specific accuracy requirements for these errors is given.

(4) This article only studied the mechanical response analysis of a 100,000 m^3 storage tank under foundation settlement, and further research can be conducted on the engineering application of different types of small crude oil storage tanks and improved evaluation methods.

Author Contributions: Conceptualization, Y.J. and X.L.; software, Y.W.; validation, J.L. All authors have read and agreed to the published version of the manuscript.

Funding: This research was funded by the National Key Research and Development Program of China, grant number. 2022YFC3070100; Young Elite Scientists Sponsorship Program by Beijing Association for Science and Technology, grant number. BYESS2023261; National Natural Science Foundation of China, grant number. 52304013; the Science and Technology Research Project of Pipechina, grant number. WZXGL202105; the Science and Technology Research Project of Pipechina, grant number. WZXGL202104; Science Foundation of the China University of Petroleum, Beijing, grant number. 2462023BJRC005 and the Science and Technology Research Project of Pipechina, grant number. CLZB202301.

Data Availability Statement: Data are contained within the article.

Conflicts of Interest: The authors declare no conflicts of interest.

References

1. Pan, J.; Liang, S. A study on the buckling behavior of in-service large open-topped oil-storage tanks. *Structures* **2021**, *29*, 211–224. [CrossRef]
2. Zhao, J.; Li, M.; Liu, S.; Dong, H. Heat transfer characteristics of oil receiving and delivering process in crude oil storage tanks. *Case Stud. Therm. Eng.* **2024**, *61*, 104994. [CrossRef]
3. Ji, S.; Cheng, Q.; Sun, W.; Qi, Y.; Wang, S. Study on optimal operation conditions in the heating process of a crude oil single-disk floating roof tank: Insights from exergy transfer analysis method. *Energy Rep.* **2023**, *9*, 3131–3147. [CrossRef]
4. Zhao, Y.; Lei, X.; Wang, Z.; Cao, Q. Buckling behavior of floating-roof steel tanks under measured differential settlement. *Thin-Walled Struct.* **2013**, *69*, 70–80. [CrossRef]
5. Alphose, Z. Liquid-containment shells of revolution: A review of recent studies on strength, stability and dynamics. *Thin-Walled Struct.* **2015**, *87*, 102–114.
6. Ozdemir, Z.; Souli, M.; Fahjan, Y. Application of nonlinear fluid–structure interaction methods to seismic analysis of anchored and unanchored tanks. *Eng. Struct.* **2010**, *32*, 409–423. [CrossRef]
7. Konstantinos, B.; Spyros, A.K. Uplift mechanics of unanchored liquid storage tanks subjected to lateral earthquake loading. *Thin-Walled Struct.* **2021**, *158*, 107145.

8. Hamid, N.; Hossein, S.; Tadeh, Z. Experimental investigation of geometrical and physical behaviors of thin-walled steel tanks subjected to local support settlement. *Structures* **2021**, *34*, 413–422.
9. Yannis, K.C.; Panagiota, T.; Takis, G.; Amalia, G.; Jacob, C.; Stéphan, U. 3D Effective stress analyses of dynamic LNG tank performance on liquefiable soils improved with stone columns. *Soil Dyn. Earthq. Eng.* **2023**, *174*, 108170.
10. Manik, M.; Sabarethinam, K. Fragility assessment of bottom plates in above ground storage tanks during flood events. *J. Loss Prev. Process Ind.* **2023**, *282*, 104579.
11. Carl, B.; Jamie, E.P. Fragility and risk assessment of aboveground storage tanks subjected to concurrent surge, wave, and wind loads. *Reliab. Eng. Syst. Saf.* **2019**, *191*, 106571.
12. Bell, R.; Iwakiri, S. comparison used in tank-failure study. *J. Geotech. Eng. Div. ASCE* **1980**, *106*, 153–169. [CrossRef]
13. Clark, J. Survey of oil tank failure. *Ann. L'Institute Belg. Pet.* **1969**, *6*, 15–24.
14. D'Orazio, T.; Duncan, J.; Bell, R. Distortion of steel tanks due to settlement of their walls. *J. Geotech. Eng. Div. ASCE* **1989**, *115*, 871–890. [CrossRef]
15. Zhang, S.; Kang, C.; Zhang, P.; Luo, J.; Shao, Y.; Wu, G.; Deng, B. Failure analysis of local settlement induced Q345R bottom plate cracking of crude oil storage tank. *Heliyon* **2022**, *8*, e11952.
16. Rajmund, L.; Eugeniusz, H. Failure of cylindrical steel storage tank due to foundation settlements. *Eng. Fail. Anal.* **2020**, *115*, 104628.
17. Min, H.; Chen, G.; Yang, P.; Hu, K.; Zhou, L.; Men, L.; Zhao, J. Multi-hazard coupling vulnerability analysis for buckling failure of vertical storage tank: Floods and hurricanes. *Process Saf. Environ. Prot.* **2022**, *161*, 528–541.
18. Li, Q.; Zhao, D.; Yin, j.; Li, Y.; Chi, P.; Han, Y.; Ansari, U.; Cheng, U. Sediment Instability Caused by Gas Production from Hydrate-bearing Sediment in Northern South China Sea by Horizontal Wellbore: Evolution and Mechanism. *Nat. Resour. Res.* **2023**, *32*, 1595–1620. [CrossRef]
19. Jonaidi, M.; Mohamed, K. Harmonic settlement effects on uniform and tapered tank shells. *Thin-Walled Struct.* **1998**, *3*, 237–255. [CrossRef]
20. Ahmed, S.; Ansourian, P. Wall thickness variation effect on tank's shape behaviour under critical harmonic settlement. *Alex. Eng. J.* **2016**, *55*, 3205–3209.
21. Sina, N.; Hossein, S. Experimental Investigation to local settlement of steel cylindrical tanks with constant and variable thickness. *Eng. Fail. Anal.* **2020**, *118*, 104916.
22. Fan, H.; Chen, Z.; Shen, J.; Cheng, J.; Chen, D.; Jiao, P. Buckling of steel tanks under measured settlement based on Poisson curve prediction model. *Thin-Walled Struct.* **2016**, *106*, 284–293. [CrossRef]
23. Chen, Z.; Fan, H.; Cheng, J.; Jiao, P.; Xu, F.; Zheng, C. Buckling of cylindrical shells with measured settlement under axial compression. *Thin-Walled Struct.* **2018**, *123*, 351–359. [CrossRef]
24. Suranga, G.; Hoyoung, S.; William, D.L.; Priyantha, W.J. Analysis of edge-to-center settlement ratio for circular storage tank foundation on elastic soil. *Comput. Geotech.* **2018**, *102*, 136–147.
25. Luis, A.G. Buckling of vertical oil storage steel tanks: Review of static buckling studies. *Thin-Walled Struct.* **2016**, *103*, 1–21.
26. Cao, Q.; Zhao, Y. Buckling strength of cylindrical steel tanks under harmonic settlement. *Thin-Walled Struct.* **2010**, *48*, 391–400. [CrossRef]
27. Gong, J.; Tao, J.; Zhao, J.; Zeng, S.; Jin, T. Buckling analysis of open top tanks subjected to harmonic settlement. *Thin-Walled Struct.* **2013**, *63*, 37–43. [CrossRef]
28. Zhao, Y.; Cao, Q.; Xie, X. Floating roof steel tanks under harmonic settlement: FE parametric study and design criterion. *J. Zhejiang Univ.* **2006**, *7*, 398–406. [CrossRef]
29. Gong, J.; Cui, W.; Zeng, S.; Jin, T. Buckling analysis of large scale oil tanks with a conical roof subjected to harmonic settlement. *Thin-Walled Struct.* **2012**, *52*, 143–148. [CrossRef]
30. Harsh, B.; Sukru, G. Fitness-for-service of open-top storage tanks subjected to differential settlement. *Eng. Struct.* **2020**, *225*, 111277.
31. Yang, Z.; Yin, L. Buckling of cylindrical open-topped steel tanks under wind load. *Thin-Walled Struct.* **2014**, *79*, 83–94.
32. Shervin, M.; Alireza, M. 3D wind buckling analysis of steel silos with stepped walls. *Thin-Walled Struct.* **2019**, *142*, 236–261.
33. Shi, L. A Study on Strength and Stability of Large Scale Crude Oil Storage Tanks. Ph.D. Thesis, China University of Petroleum, Beijing, China, 2016.
34. Grget, G.; Ravnjak, K.; Szavits, A. Analysis of results of molasses tanks settlement testing. *Soils Found.* **2018**, *58*, 1260–1271. [CrossRef]

Disclaimer/Publisher's Note: The statements, opinions and data contained in all publications are solely those of the individual author(s) and contributor(s) and not of MDPI and/or the editor(s). MDPI and/or the editor(s) disclaim responsibility for any injury to people or property resulting from any ideas, methods, instructions or products referred to in the content.